

MICROWAVE TECHNIQUES FOR NDE OF CERAMICS

A. J. Bahr
SRI International
Menlo Park, California 94025

ABSTRACT

In recent years, the technology for generating and controlling electromagnetic energy at frequencies of 100 GHz and above has improved considerably, and such components are now readily available. In view of this fact, we have undertaken a program to assess the applicability of this technology to the NDE of ceramic materials and components. We have found that Si_3N_4 is nearly transparent at these high frequencies, which permits the interior of components made from this material to be inspected using microwave energy. The dielectric constant of hot-pressed Si_3N_4 is about 7.5, so the wavelength in this material at 100 GHz is about 1mm. This electromagnetic wavelength is comparable to the acoustic wavelength of 10 MHz ultrasound in this material. Thus, microwave C-scan images will have resolutions roughly comparable to those produced by commercial ultrasonic equipment, but do not require the use of a water bath or other coupling medium in order to achieve rapid scanning. In addition, electromagnetic and ultrasonic scattering will differ for a given flaw, and thus microwave imaging may provide better flaw discrimination in some cases.

Cross-Polarized Transmission Measurements

A block diagram of our experimental arrangement is shown in Fig. 1. The ceramic samples are translated between the sensors in the X-direction via a motor-driven stage, and incrementally in the Y-direction by means of a micrometer positioner.

Broad-flange, open-ended waveguides were used to achieve broadband operation. Since the backward-wave oscillator is capable of being swept over a wide frequency range, we were able to determine the best operating frequency in the neighborhood of 100 GHz for each type of inclusion. Typical frequency responses for four important types of inclusions are shown in Fig. 2. The nominal diameter of these inclusions is 0.020 inches. We note that there are significant variations in these frequency responses, and this fact may prove useful for flaw identification. However, these frequency responses are determined in part by the reflections from the surfaces of the ceramic plate containing the inclusions, and thus it may be difficult to separate the flaw-dependent information from these responses.

C-Scan of Plates

Three different plates of Norton hot-pressed NC 132 containing seeded inclusions and voids were examined using the cross-polarized transmission technique. Figure 3 shows a C-scan of a portion of a plate containing 0.020" and 0.005" inclusions of WC, Fe, Si, and C. Figure 3(a) shows the area covered by the scan and the intended flaw locations. Figure 3(b) shows the portions of the scan area that produce a scattered signal greater than an arbitrarily selected threshold value. Finally, Fig. 3(c) shows the amplitude of the scattered signal as a function of position within the scan area.

Several features of this C-scan are noteworthy. First, all 0.020" flaws are detected. Iron provides the strongest signal, and is the only 0.005" flaw that is clearly detected in this figure. (The other small flaws become more apparent if the frequency is changed.) Second, X-rays show that diffusion of the iron inclusion during hot pressing produces an irregularly shaped scatterer that causes the spatial extent for this flaw to appear overly large in the microwave C-scan. Finally, it appears that a crack-like flaw is present between the 0.020-inch diameter iron and silicon inclusions. Apparently, X-ray, ultrasonic, and dye-penetrant examination by AMMRC did not reveal the presence of such a flaw. If this flaw is indeed found to be real, it would indicate the superior sensitivity of the microwave technique for detecting this type of flaw.

Figure 4 shows a similar microwave C-scan, but for a Si_3N_4 plate containing different types and densities of inclusions. All of the 0.005" inclusions are detected in this scan, but, of course, the closer spacing between inclusions may enhance this detection.

In Fig. 5 we see another scan of the same plate as in Fig. 4, but of only the area containing the 0.001" through 0.010"-diameter silicon inclusions. The sensitivity of our technique for the detection of unreacted silicon appears to be good, and may be better for this purpose than other techniques. This feature could be important in a process-control application.

The data shown in Fig. 6 demonstrates our ability to detect small voids in Si_3N_4 , as well as inclusions. The voids were formed in the interior of a 0.250"-thick plate by first drilling small holes in a 0.125"-thick plate, and then diffusion bonding this plate to a second 0.125"-

thick plate. The voids that were not detected by microwaves were also weakly imaged in an X-ray, indicating that these particular holes probably contained some kind of material.

It is interesting to note that partial diffraction pattern produced by the uppermost holes on the left of the scan area. In principle, such a diffraction pattern could provide information about the geometry of the scatterer. The microwave C-scan apparently also shows some inclusions that are not detected in the ultrasonic C-scan.

C-Scan of a Disk

A hot-pressed Si_3N_4 billet in the form of a disk was also examined using microwaves. The main reason for examining this disk was to make a qualitative determination of the effect of the grit-blasted, as-pressed surface on the microwave C-scan. The results obtained before and after the surface of the disk was ground smooth are shown in Fig. 7. The frequency was 94.4 GHz. It can be seen that this amount of surface roughness begins to contribute a significant level of background clutter at this frequency.

After the surface was ground smooth, a microwave C-scan of the disk was made that extended over the edges of the disk. These results are shown in Fig. 8. X-rays showed the presence of an unintended high-density inclusion in the disk, and this flaw is detected in the microwave C-scan. This experiment also shows the effect of diffraction near a sharp edge. The cross-polarized scattering from an edge is quite strong, and can be detected at a significant distance from the edge. Qualitatively, we can conclude that flaws near a sharp edge will not be detected with this technique.

Acknowledgement

This work was sponsored by the Army Materials and Mechanics Research Center under Contract DAAG46-76-C-0048.

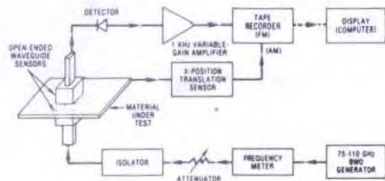


Figure 1. Experimental arrangement for cross-polarized transmission measurements.

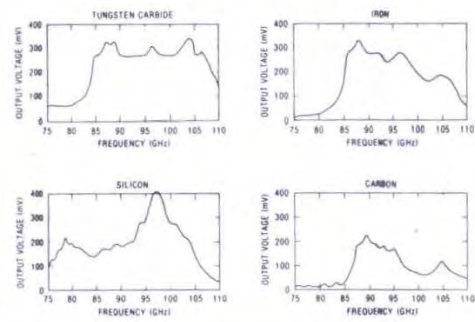


Figure 2. Frequency dependence of the cross-polarized forward scattering from four types of inclusions in a hot-pressed Si_3N_4 plate.

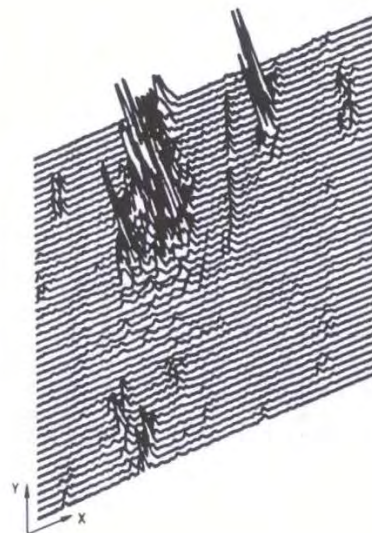
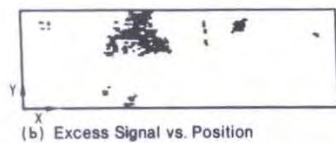
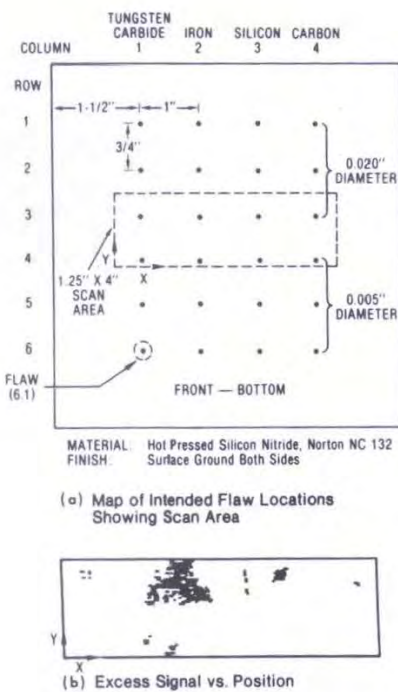


Figure 3. Microwave cross-polarized-transmission C-scan of four types of inclusions in Si_3N_4 (frequency = 94 GHz).

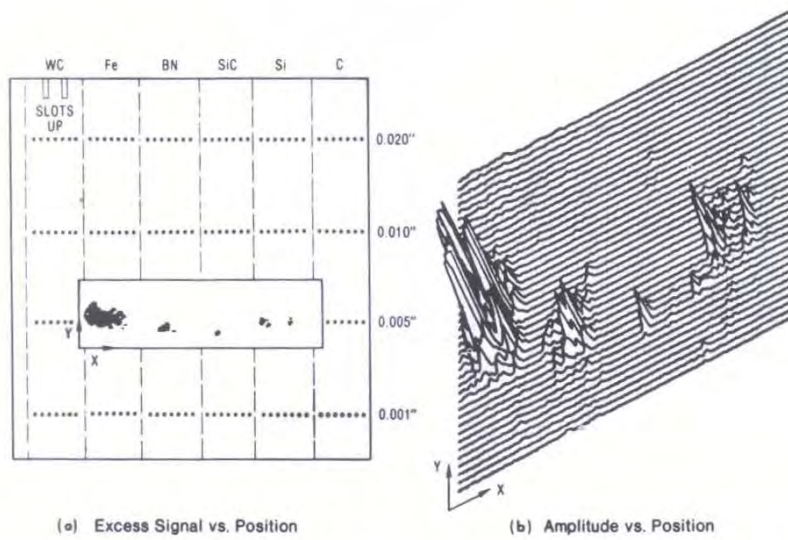


Figure 4. Microwave cross-polarized-transmission C-scan of four types of inclusions in Si_3N_4 (frequency = 91 GHz).

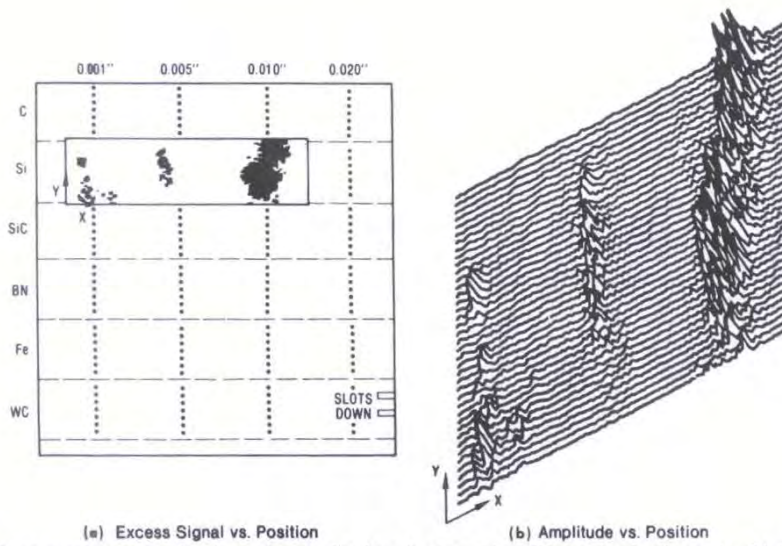
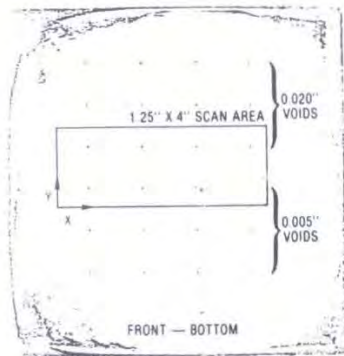
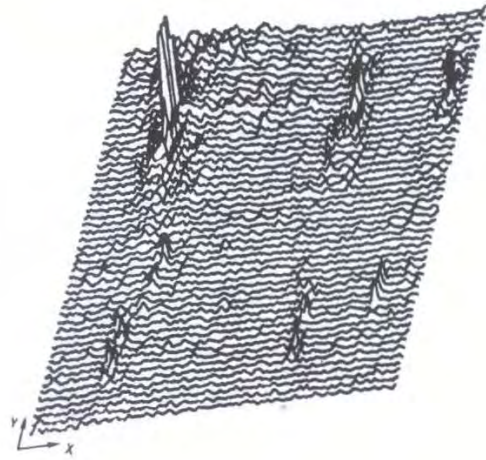


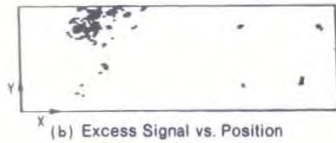
Figure 5. Microwave cross-polarized-transmission C-scan of silicon inclusions in Si_3N_4 (frequency = 98 GHz).



(a) Ultrasonic C-Scan (Focussed 25 MHz) Map Showing Void Locations and Scan Area



(c) Amplitude vs. Position



(b) Excess Signal vs. Position

Figure 6. Microwave cross-polarized-transmission C-scan showing voids in Si_3N_4 (frequency = 94 GHz).

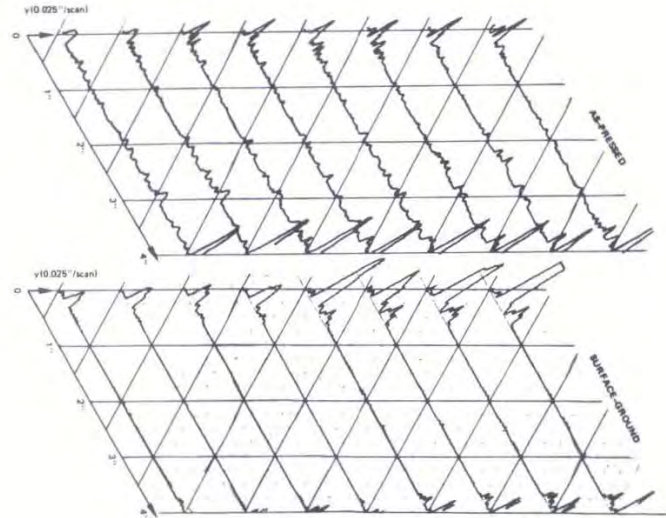
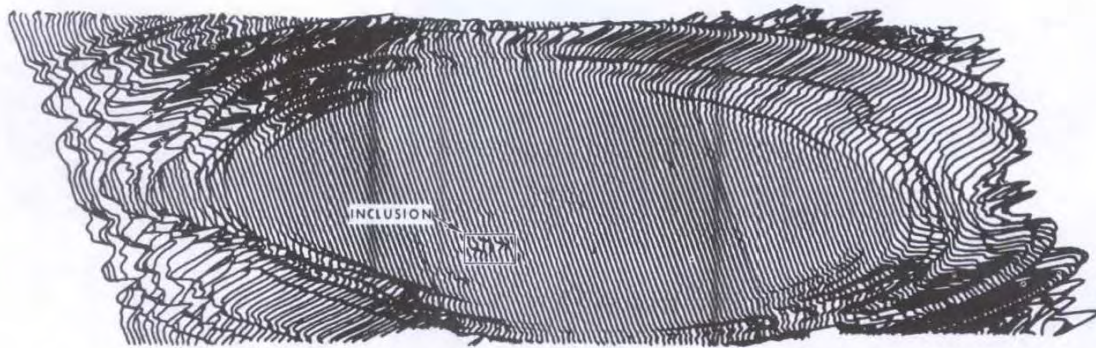
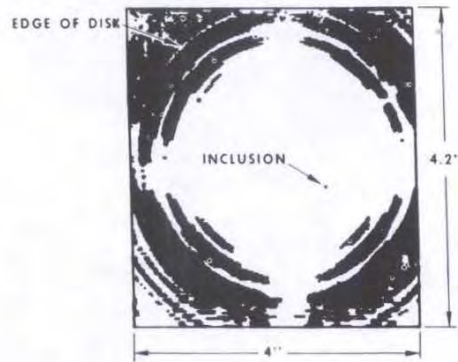


Figure 7. Effect of surface roughness.



(a) Amplitude vs. position



(b) Excess signal vs. position

Figure 8. Microwave cross-polarized-transmission C-scan of 4"-diameter hot-pressed Si_3N_4 disk (frequency = 94.4 GHz).